# BIFURCATIONS IN A CAR-FOLLOWING MODEL WITH DELAY

**Gábor Orosz** [*], **R. Eddie Wilson** [*], **Bernd Krauskopf** [*]

[*] *Bristol Centre for Applied Nonlinear Mathematics, Department of Engineering Mathematics, University of Bristol, Bristol BS8 1TR, United Kingdom*

Abstract: A simple car-following model that includes the reaction time of drivers is analyzed by numerical continuation techniques for the case of five cars on a ring. A two-dimensional bifurcation diagram is computed that summarizes the dynamics of steady states, oscillating solutions, collisions, and stopping as a function of model parameters. Further, a mechanism is proposed by which different spatial patterns may appear. 

Keywords: vehicle dynamics, nonlinear analysis, bistability

## 1. INTRODUCTION

In this paper a car-following model of highway traffic is studied which regards vehicles as discrete entities moving in continuous time and one-dimensional space. Furthermore, the model incorporates delay due to the drivers' *reaction time*.

Specifically, an *Optimal Velocity model* is considered, which was first presented without delay in (Bando *et al.*, 1995). The delay was first added in (Bando *et al.*, 1998). The model introduced in Section 2 has recently been investigated by Davis (2002; 2003) with linear analysis and numerical simulation to find stable solutions. Note that there exist other delayed car-following models which can be either simple like in (Holland, 1998), or highly complicated like in (Wilson, 2001).

The first systematic global study of stable and unstable solutions was presented in (Orosz *et al.*, 2004) for the case of $n = 3$ vehicles driving on a circular road. The extension of that work to a larger number of cars is necessary because real traffic situations comprise hundreds, or even thousands of cars. As a first step in the large $n$ direction, here the case of $n = 5$ cars is studied to find more complicated patterns along the ring. The main tool is numerical bifurcation analysis with DDE-BIFTOOL and customized routines to find collisions and stopping.

## 2. THE MODEL

For the sake of simplicity, drivers have identical characteristics and they react only to the motion of the car ahead. The vehicles' positions are denoted by $x_i$, their velocities by $v_i$, and their relative displacements (called *headways*) by $h_i$. Further, it is assumed that drivers do not react instantaneously to their headways but after a reaction time delay $\tau$, which is also taken to be the same for all drivers. A simple model for the acceleration of the $i$-th vehicle can be given by the dimensionless equations

$$\dot{v}_i(t) = \alpha \left[ \mathrm{V}\left(h_i(t-1)\right) - v_i(t) \right] , \qquad (1)$$

which, together with the kinematic conditions

$$\dot{h}_i(t) = v_{i+1}(t) - v_i(t) , \qquad (2)$$

constitute a system of delay differential equations (DDEs) for the vehicles' motions. Here the dot

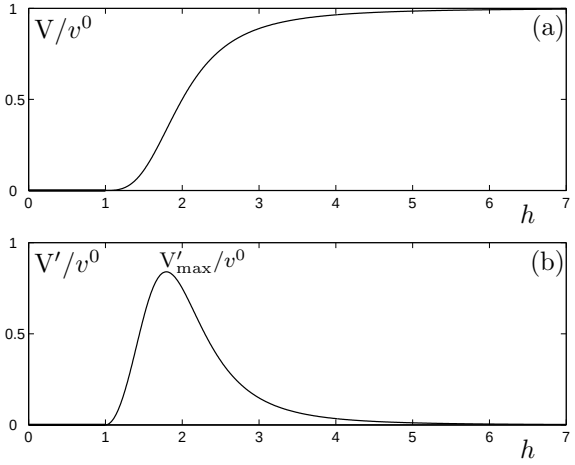


Fig. 1. The rescaled Optimal Velocity function $\mathrm{V}(h)$ (a), and its first derivative with respect to $h$ (b).

denotes derivation with respect to time, $\tau$ is rescaled to 1, $\alpha > 0$ is known as the *sensitivity*, and $\mathrm{V}(h)$ is an *Optimal Velocity function*. The function $\mathrm{V}(h)$ prescribes how the drivers adjust their velocity as a function of the headway in front of them.

In this paper, we assume the rescaled OV function

$$\mathrm{V}(h) = \begin{cases} 0 & 0 \le h \le 1\,, \\ v^0 \dfrac{(h-1)^3}{1+(h-1)^3} & h > 1\,. \end{cases} \tag{3}$$

It is depicted in Fig. 1(a) and its first derivative with respect to $h$ is shown in Fig. 1(b). The function (3) clearly has the following features:

- $\mathrm{V}(h)$ is continuously differentiable, non-negative, and monotone increasing.
- $\mathrm{V}(h) \to v^0$ as $h \to \infty$, where the *desired speed* $v^0$ corresponds to the speed limit.
- $\mathrm{V}(h) \equiv 0$ over the interval $h \in [0, 1]$, where 1 is the rescaled *jam headway*.

For more information about the modelling see (Orosz *et al.*, 2004).

The case of five cars on a circular road is considered here. The *uniform flow equilibrium* of the OV model (1)–(2) is

$$h_i(t) \equiv h^* = L/5\,, \quad v_i(t) \equiv \mathrm{V}(h^*)\,, \tag{4}$$

for $i = 1, \ldots, 5$, where $L$ is the length of the circular road and $h^*$ is called the *average headway*. The linear stability of this solution is analyzed in the next section. When it loses its stability then wave patterns may appear. Note that numerical continuation can be applied to the OV model (1)–(2) with OV function (3), because it satisfies the required smoothness features.

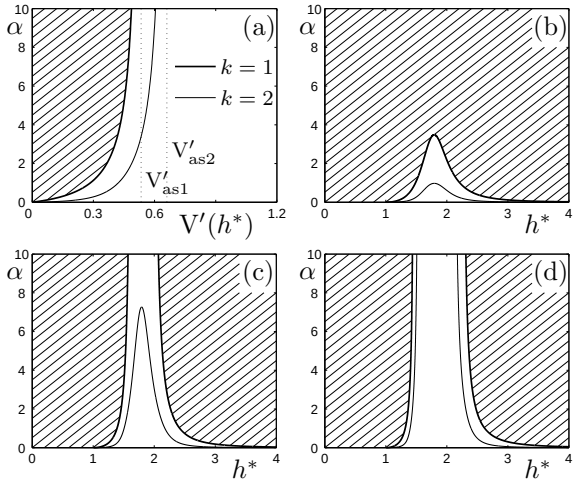


Fig. 2. Stability charts of the five-car system where shading denotes the stable region. Panel (a) shows the sensitivity $\alpha$ as a function of the slope of the OV function $\mathrm{V}'(h^*)$. Panels (b)–(d) show stability diagrams in the $(h^*, \alpha)$-plane, namely panel (b) for $v^0 = 0.5$, panel (c) for $v^0 = 0.7$, and panel (d) for $v^0 = 1.0$.

## 3. LINEAR STABILITY ANALYSIS

The linear stability of the DDE model about the equilibrium (4) is analyzed now. By computing the Hopf bifurcation curves it is possible to predict what kind of patterns can appear in the system.

Analyzing the linear part of (1)–(2) one may obtain the Hopf curves in the form

$$\begin{aligned} \mathrm{V}'(h^*) &= \frac{\omega}{2\cos(\omega - k\pi/5)\sin(k\pi/5)}\,, \\ \alpha &= -\omega\cot(\omega - k\pi/5)\,, \end{aligned} \tag{5}$$

where $k = 1, \ldots, 4$ is introduced by taking the fifth root of unity. Furthermore, it can be shown that the spatial pattern along the ring is described by the discrete waves

$$s_i = \cos\left(\frac{2\pi k}{5} i\right), \tag{6}$$

for $i = 1 \ldots 5$. Therefore $k$ can be considered as the discrete spatial wavenumber of oscillations. Note that the cases $k = 1$ and $k = 3$ describe one wave along the ring, whereas the cases $k = 2$ and $k = 4$ describe two waves along the ring; see (Orosz *et al.*, 2004).

One may show that the left most curve in the $(\mathrm{V}'(h^*), \alpha)$-plane is described by (5) with $k = 1$. This is depicted by a solid bold curve in Fig. 2(a). This curve is qualitatively the same as for the case $n = 3$, but now it is parameterized by $\omega \in (0, \pi/5)$ and possesses a vertical asymptote at $\mathrm{V}'_{\mathrm{as1}} \simeq 0.5345$.

However, for five cars there is an additional curve belonging to the wavenumber $k = 2$ to the right of the curve for $k = 1$. It is parameterized by $\omega \in (0, 2\pi/5)$ and has the vertical asymptote $V'_{as2} \simeq 0.6607$; see the solid thin curve in Fig. 2(a).

Using stability criteria for DDEs (Stépán, 1989), it can be shown that the uniform flow equilibrium (4) is asymptotically stable to the left of the $k = 1$ curve (shaded region in Fig. 2(a)) and linearly unstable otherwise. This is similar to the case $n = 3$. When crossing the curves for $k = 1$ and $k = 2$ from the left to the right, Hopf bifurcations take place. However, the second Hopf bifurcation does not change the stability of the steady state, but rather moves spectra to the right of the imaginary axis, giving a region with four unstable eigenvalues.

To convert Fig. 2(a) to diagrams in the $(h^*, \alpha)$-plane of average headway and sensitivity one uses the fact that the derivative $V'(h)$ of the OV function (3) possesses a single maximum over the interval $h \in [1, \infty)$, as shown in Fig. 1(b). The Hopf curves belonging to wavenumbers $k = 1$ and $k = 2$ may be closed above or may possess vertical asymptotes in the $(h^*, \alpha)$-plane, depending on the relation of their asymptotes $V'_{as1,2}$ and the maximum of the derivative $V'_{max} \simeq 0.8399\, v^0$, so that three qualitatively different diagrams can be obtained.

- For $V'_{max} < V'_{as1}$, that is, for $v^0 < 0.6363$, two single Hopf curves exist, each with a maximum; see Fig. 2(b).
- For $V'_{as1} < V'_{max} < V'_{as2}$, that is, for $0.6363 < v^0 < 0.7865$, there are two Hopf curves for $k = 1$ with vertical asymptotes, but the curve for $k = 2$ is still a single curve; see Fig. 2(c).
- Finally, for $V'_{max} > V'_{as2}$, that is, for $v^0 > 0.7865$, there are four Hopf curves, all possessing vertical asymptotes; see Fig. 2(d).

Note that without delay the Hopf curves in the $(V'(h^*), \alpha)$-plane are straight lines with the slopes $2\cos^2(k\pi/5)$, which always result in closed curves in the $(h^*, \alpha)$-plane as in Fig. 2(b); *e.g.*, see (Sugiyama and Yamada, 1998).

The new feature for the case of five cars considered here is the second Hopf curve for the wavenumber $k = 2$.

By considering the nonlinear terms of (1) up to order three, the type of the Hopf bifurcation and the approximate amplitude of the oscillating solution can be determined analytically; see (Orosz *et al.*, 2004).

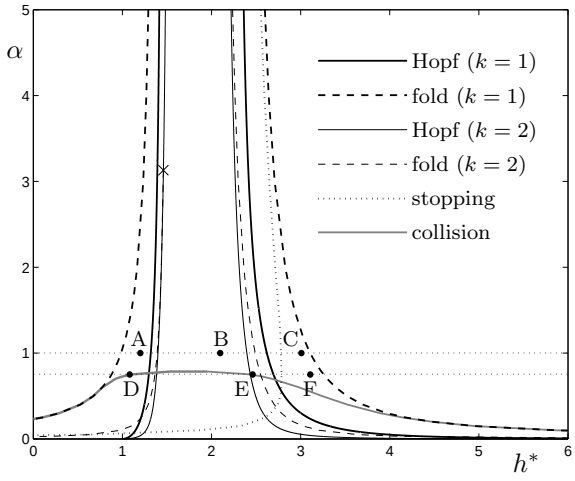


Fig. 3. Two-dimensional bifurcation diagram. The horizontal dotted lines correspond to the values of $\alpha$ used in Fig. 4 and the marked points A–F correspond to the respective time profiles in Fig. 5

## 4. THE BIFURCATION DIAGRAM

The global behavior of the DDE model (1)–(2) in the $(h^*, \alpha)$-plane can be investigated with the Matlab package DDE-BIFTOOL; see (Engelborghs *et al.*, 2001).

First, the branch of steady states is continued as a function of the parameter $h^*$, to obtain a numerical approximation of (4). Hopf bifurcations are detected on this branch when a complex conjugate pair of eigenvalues crosses the imaginary axis. The Hopf curves found in Section 3 can be followed in the $(h^*, \alpha)$-plane.

The branch of oscillating solutions arising from the Hopf point is continued as a function of $h^*$ and fold bifurcations of oscillating solutions are detected when a Floquet multiplier cross the unit circle at $+1$. Presently, DDE-BIFTOOL is unable to follow fold bifurcations in the $(h^*, \alpha)$-plane. Therefore a script was used that finds the fold points and also the points where vehicles stop and collide for the first time. (Since numerically the velocity never reaches zero, stopping is detected by setting a small positive threshold, in this case 0.01.)

It is possible to execute this process for several values of the parameter $\alpha$ which results in boundaries in the $(h^*, \alpha)$-plane. To obtain smooth curves about 30 points are computed along each boundary. It is very time consuming to obtain these curves with good resolution for a large number of cars (even $n = 5$ is quite large in this respect), that is, for a DDE consisting of many component equations; see (Engelborghs *et al.*, 2002) for more information about the cost and complexity of the numerical methods.

The two-dimensional bifurcation diagram is displayed in Fig. 3 for the case $v^0 = 1$, *i.e.*, as in Fig. 2(d). The Hopf curves are depicted by solid and the fold curves by dashed lines. These are shown as bold and thin curves for $k = 1$ and $k = 2$, respectively.

The regions between the outer Hopf and outer fold curves are bistability regions, where a stable steady state coexists with a stable oscillating solution which belongs to $k = 1$. This behavior has been found in the case $n = 3$ (Orosz *et al.*, 2004), but now these regions are larger. Additionally, similar regions exist between the inner Hopf and inner fold curves, but here the steady state and the oscillating state (now belonging to $k = 2$) are already unstable.

The grey curve represents the first collision; cars collide below the curve. The dotted curve represents the first stopping; vehicles stop between this and the left most fold curve. These domains have also been found in the three-car case (Orosz *et al.*, 2004), but in Fig. 3 they are quite a bit larger.

All of the depicted curves have vertical asymptotes, except for the collision curve and the left fold curve for $k = 2$ which ends at a degenerate Hopf point (denoted by $\times$). The Hopf bifurcations are always subcritical, except along the section above the degenerate point. This behavior is typical for a situation of sufficiently large $v^0$, as in Fig. 2(d) and Fig. 3.

The overall picture is the following. When increasing the number of cars the bistability, collision, and stopping domains become larger and appear to converge quickly to a limit as $n \to \infty$. This remains conjectural at this point, but is supported by the analytical and numerical results presented here.

### *4.1 One-dimensional cross sections*

To demonstrate important behaviors such as collision and stopping, we present the continued branch of oscillating solutions for some particular values of $\alpha$, namely along the horizontal cross sections indicated in Fig. 3 by dotted horizontal lines.

The results are shown in Fig. 4 for $\alpha = 1$ and $\alpha = 0.75$. The horizontal axis represents the equilibrium state, while the branches of oscillating solutions are represented by the amplitude of oscillations $v_i^{\mathrm{amp}} = (v_i^{\max} - v_i^{\min})/2$, $(i = 1, \ldots, 5)$ of the vehicles' velocities. When the solution is stable (unstable) the corresponding branch is plotted as a solid (dashed) curve. Furthermore, the branches belonging to $k = 1$ and $k = 2$ are plotted as bold and thin curves, respectively.

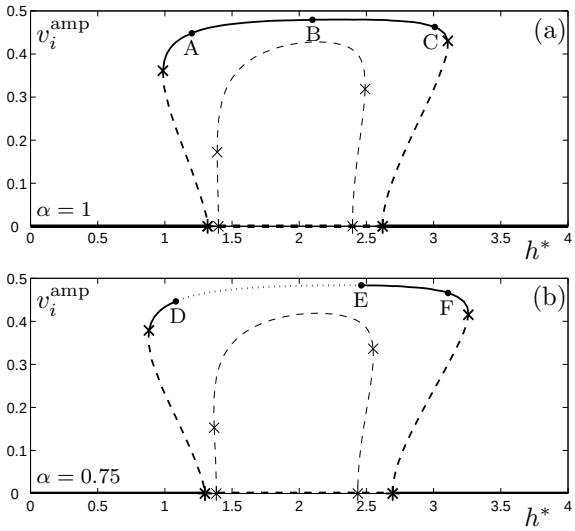


Fig. 4. Amplitude of oscillations of the velocity of the $i$-th car vs. average headway $h^*$. The horizontal axis represents the equilibrium state. Solid curves denote stable and dashed curves denote unstable states; the dotted curve represents the collision region. The bold and thin curves belong to the cases $k = 1$ and $k = 2$, respectively. The value of $\alpha$ is depicted in each panel and $v^0 = 1$ for both (a) and (b).

The branch of equilibria is unstable between two outer Hopf bifurcations (denoted by *****). The inner Hopf bifurcations (denoted by *) change the stability of the equilibrium in accordance with the results shown in Fig. 2(d).

In Fig. 4(a), for $\alpha = 1$, two branches of oscillating solutions are depicted belonging to the wavenumbers $k = 1$ (outer bold curve) and $k = 2$ (inner thin curve). The outer curve starts at the outer Hopf points and then folds back to constitute a stable oscillating branch (the fold points are denoted by $\times$). This leads to bistability regions where the coexisting stable steady state and stable oscillating solution are separated by an unstable oscillating solution.

The inner curve of oscillating solutions behaves similarly to the outer one. However, it is always unstable because one of the Floquet multipliers belonging to this branch is always outside the unit circle while another multiplier governs the folding when crossing the unit circle at $+1$. Therefore, on the regions situated on both sides of this branch only unstable solutions coexist.

Three points A–C on the stable oscillating branch in Fig. 4(a) are marked and are also shown in Fig. 3. The associated time profiles of velocities (solid curves) and headways (dashed curves) over one oscillation period for the first car are displayed in Fig. 5(a)–(c). (These plots are the same for all cars, except for a time shift.) The velocity reaching zero corresponds to stopping of vehicles.

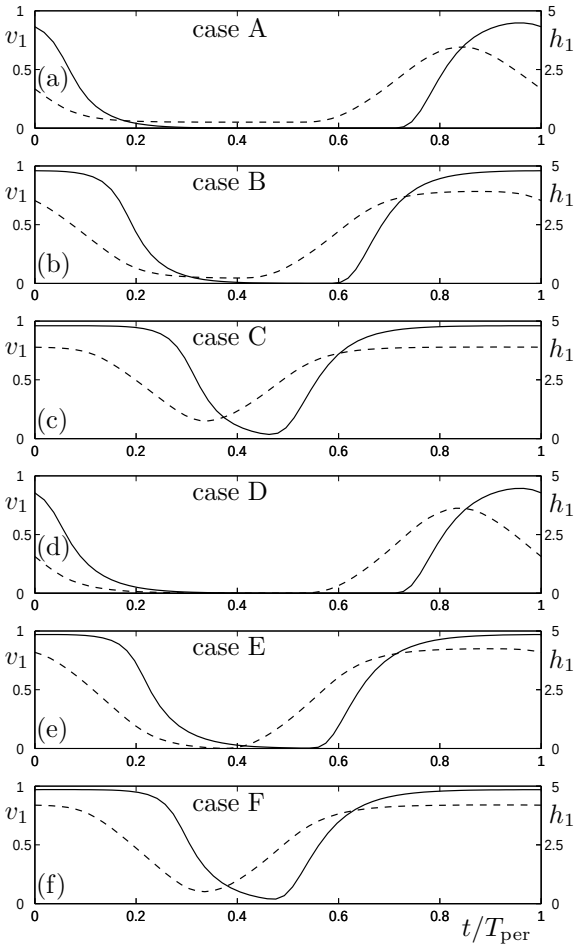


Fig. 5. Oscillations of the velocity of the first car over one period, shown as solid curves to the scale on the left; oscillations of the headway of the first car over one period, shown as dashed curves to the scale on the right. Cases A–F correspond to the marks in Fig. 3 and Fig. 4.

When the headway reaches zero then cars touch each other, which corresponds to a collision. When the headway crosses zero then vehicles 'move through' each other; the model becomes invalid when this occurs.

Comparing the velocity profiles of cases A–C, one may see that cars nearly reach the desired speed $v^0 = 1$ in cases B and C, and stop in cases A and B. Furthermore, the stopping region is more extended in case A than in case B. For the headways the profiles are similar, although these do not reach zero, that is, cars do not collide. Finally, stopping and accelerating always occurs later than the drop and increase of the headway. This is an obvious consequence of the delay.

In Fig. 4(b), for $\alpha = 0.75$, the bifurcation diagram is qualitatively the same as in Fig. 4(a), but the bistability region is wider. Furthermore, the headway crosses zero during its oscillation along the dotted section of the oscillating branch. Decreasing $\alpha$ further, the collision extends all over the stable part of the branch when the grey collision curve reaches the outer fold curves in Fig. 3.

Three points D–F are marked on the branch of stable oscillating solutions in Fig. 4(b) and are also displayed in Fig. 3. The respective profiles of velocities and the headways are presented in Fig. 5(d)–(f). The stopping process is qualitatively the same as in cases A–C, but now the headway becomes zero for cases D and E (first collision) corresponding to the fact that these points are on the collision curve in Fig. 3. The headway crosses zero for the parameter values of $h^*$ between D and E.

## 5. CONCLUSION AND FUTURE WORK

The car-following model presented here is valid for any number of cars, but the numerical bifurcation analysis becomes very expensive as $n$ is increased. Here the case of five cars is presented as the first extension of the bifurcation analysis of the model with more than one wavenumber. These results could be extended to the case of larger $n$ when there are many nested Hopf curves. When increasing the number of cars, the upper part of the oscillation branches belonging to $k = 2, 3, \ldots$ extend to the $k = 1$ branch, so that their unstable Floquet multipliers are in close neighborhood of the unit circle. This results in weakly unstable oscillations with slowly decaying motion in these wavenumbers. This phenomenon will be discussed in detail elsewhere.

Finally, we mention that the limit of $n \to \infty$ gives rise to a continuum model in the form of a partial differential equation with delay. At present continuum models of car following, such as (Berg *et al.*, 2000), have only been studied without the effect of delay due to the drivers' reaction time. Indeed, developing and studying continuum models with delay remains a considerable challenge for future research.

## REFERENCES


Bando, M., K. Hasebe, A. Nakayama, A. Shibata and Y. Sugiyama (1995). Dynamical model of traffic congestion and numerical simulation. *Physical Review E* **51**(2), 1035–1042.

Bando, M., K. Hasebe, K. Nakanishi and A. Nakayama (1998). Analysis of optimal velocity model with explicit delay. *Physical Review E* **58**(5), 5429–5435.

Berg, P., A. Mason and A. Woods (2000). Continuum approach to car-following models. *Physical Review E* **61**(2), 1056–1066.

Davis, L. C. (2002). Comment on "Analysis of optimal velocity model with explicit delay". *Physical Review E* **66**(3), 038101.

Davis, L. C. (2003). Modification of the optimal velocity traffic model to include delay due to driver reaction time. *Physica A* **319**, 557–567.

Engelborghs, K., T. Luzyanina and D. Roose (2002). Numerical bifurcation analysis of delay differential equations using DDE-BIFTOOL. *ACM Transactions on Mathematical Software* **28**(1), 1–21.

Engelborghs, K., T. Luzyanina and G. Samaey (2001). DDE-BIFTOOL v. 2.00: a Matlab package for bifurcation analysis of delay differential equations. Technical Report TW-330. Department of Computer Science, Katholieke Universiteit Leuven, Belgium. (`http://www.cs.kuleuven.ac.be/~koen/delay/ddebiftool.shtml`).

Holland, E. N. (1998). A generalized stability criterion for motorway traffic. *Transportation Research Part B: Methodological* **32**(2), 141–154.

Orosz, G., R. E. Wilson and B. Krauskopf (2004). Global bifurcation investigation of an optimal velocity traffic model with driver reaction time. *Physical Review E* **70**(2), 026207.

Stépán, G. (1989). *Retarded Dynamical Systems: Stability and Characteristic Functions*. Vol. 210 of *Pitman Research Notes in Mathematics*. Longman, Essex, England.

Sugiyama, Y. and H. Yamada (1998). Aspects of optimal velocity model for traffic flow. In: *Traffic and Granular Flow '97* (M. Schreckenberg and D. E. Wolf, Eds.). Springer-Verlag, Singapore. pp. 301–318.

Wilson, R. E. (2001). An analysis of Gipps's car-following model of highway traffic. *IMA Journal of Applied Mathematics* **66**(5), 509–537.